Vietnam Journal of Earth Sciences, 45(1), 33-48, https://doi.org/10.15625/2615-9783/17568

Vietnam Journal of Earth Sciences
https://vjs.ac.vn/index.php/jse

Effects of physical properties and undrained cyclic shear conditions on the pore water pressure responses of saturated sands and clays

Tran Thanh Nhan[1]*, Hiroshi Matsuda[2], Tran Thi Phuong An[1], Nguyen Thi Thanh Nhan[1], Pham Van Tien[3], Do Quang Thien[1]

[1]*University of Sciences, Hue University, 77 Nguyen Hue, Hue, Vietnam*
[2]*Yamaguchi University, 2-16-1 Tokiwadai, Ube, Yamaguchi, 755-8611, Japan*
[3]*Institute of Geological Sciences, VAST, Hanoi, Vietnam*

Received 6 June 2022; Received in revised form 8 September 2022; Accepted 10 October 2022

ABSTRACT

For clarifying the effects of relative density (D_r) and Atterberg's limits on the cyclic shear-induced pore water pressure properties of soils, sandy soils with similar index properties and clayey soils with different Atteberg's limits were collected from Vietnam and Japan and used for this study. Specimens at D_r = 50% of Nam O sand and D_r = 70% of Toyoura sand, and those of Hue clay and Japanese Kaolin clay were consolidated under the vertical stress of σ_{vo} = 49 kPa. They were then subjected to undrained cyclic shear for various cyclic shear directions and wide ranges of the number of cycles and shear strain amplitudes. Under the same cyclic shearing conditions, specimens of sand at higher D_r (Toyoura sand) and clay with higher Atterberg's limits (Kaolin) show a lower pore water pressure ratio. The number of cycles and the cumulative shear strain at the starting point of pore water pressure generation were observed for different soils and testing conditions. In addition, using the cumulative shear strain, a new strain path parameter, the effects of shear strain amplitude and cyclic shear direction can be captured, resulting in a unique u_{acc}/σ'_{vo} - G^* relation on each soil. Based on this, fitting lines can be drawn and referred to promote a prediction of the cyclic shear-induced pore water pressure accumulation for the used soils under different cyclic shear conditions.

Keywords: Atterberg's limits, clay, cyclic shear condition, pore water pressure, relative density, sand.

1. Introduction

Under undrained cyclic shear, no permanent pore water pressure remains after cyclic loading when the applied amplitude is smaller than a specific threshold value. The cyclic shear strain amplitude (γ) that divides the domains with no pore water pressure accumulation and significant accumulation is called the threshold cyclic shear strain (γ_{tp}), when $\gamma > \gamma_{tp}$, continuous and rapid accumulation of cyclic shear-induced pore water pressure (u_{acc}) is observed with the number of cycles (n). In contrast, when $\gamma < \gamma_{tp}$, such accumulation of u_{acc} is negligible even after many cycles (Hsu and Vucetic, 2006). γ_{tp} is considered a fundamental property of the cyclic behavior of saturated soils subjected to undrained cyclic loading and is visually defined as an illustration given by Hsu and Vucetic (2006) in Fig. 1.

*Corresponding author, Email: ttnhan@hueuni.edu.vn

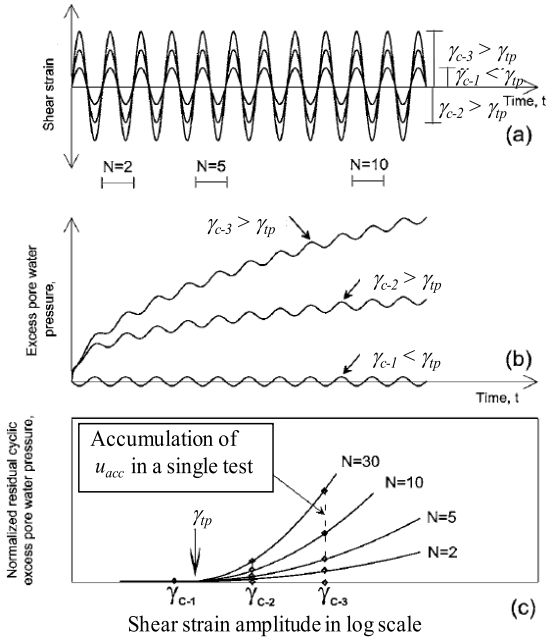

Figure 1. Definition of the threshold shear strain amplitude for pore water pressure buildup (Hsu and Vucetic, 2006)

For sandy soils, γ_{tp} has been investigated and mentioned in different researches. By using the strain-controlled cyclic direct simple shear test on compacted dried sand, Youd (1972), Silver and Seed (1971), and Pyke et al. (1975) suggested the value of $\gamma_{tp} \approx 0.01\%$ and below which no change in volume occurs. Dobry et al. (1982) demonstrated the existence of the same value $\gamma_{tp} \approx 0.01\%$ and below which no pore water pressure develops in saturated sand. The concept of γ_{tp} was used to predict the liquefaction potential and develop a model for pore pressure buildup in saturated sands (Dobry et al., 1980; 1985). On the contrary, a few studies directly or indirectly dealing with the concept of γ_{tp} were carried out for clays. Based on the stress-controlled cyclic triaxial test on saturated clay, Matsui et al. (1980) proposed a value of $\gamma_{tp} \approx 0.1\%$ for normally consolidated clay (NC clay). Later, by conducting several series of undrained uniform and irregular cyclic simple shear tests on saturated NC Kaolin, Ohara and Matsuda (1987; 1988; 1989) and Matsuda et al. (1991) indicated that the pore water pressure starts to increase when $\gamma \geq 0.05\%$ and the significant changes at $\gamma = 0.1\%$. Based on six cyclic NGI-type DSS constant volume equivalent undrained tests on one sand, two elastic silts, and one clay, Hsu and Vucetic (2006) indicated that cohesive soils show a larger value of γ_{tp} than those obtained on cohesionless soils and that γ_{tp} generally increases with the plasticity index (I_p) of cohesive soils, namely γ_{tp} increases from 0.024% to 0.06% when I_p increases from 14 to 30 meanwhile for sand and gravels, γ_{tp} becomes smaller, changing in the range from 0.01 to 0.02%.

Based on several series of uni-directional and two-directional cyclic shear tests on normally and over-consolidated clays (NC and OC clays), Matsuda et al. (2015) indicated that γ_{tp} induced by the two-directional cyclic shear increases from 0.1% to 0.2% for the range of OCR from 2 to 5 and is smaller than those induced by the uni-directional cyclic shear which had been confirmed to increase from 0.05% to 0.29% for OCR from 1 to 6 by Matsuda and Ohara (1989). In addition, since the relative density and the Attergerg's limits have been confirmed in significantly affect the dynamic behavior of soils subjected to different cyclic shear conditions and models (Matsuda et al., 2011; 2012; Vucetic and Dobry, 1991), the threshold number of cycles and cumulative shear strain for pore water pressure generation and buildup have been generally compared between different soils (Nhan et al., 2012; Nhan and Matsuda, 2020) and initially clarified in more detail for Nam O sand and Hue clay (An et al., 2022). Therefore, in this study, the pore water pressure properties, including such parameters for pore water pressure generation in these soils, were further observed and compared with those obtained on Toyoura sand and Kaolin clay which have been widely used for laboratory testing and study in Japan.

2. Cyclic simple shear test

2.1. Test apparatus and specimen preparation

The multi-directional cyclic simple shear test apparatus including the situation of soil specimen in the shear box are shown in Fig. 2. The outline of the test device is shown in Fig. 3a, and the deformation model of the specimen under uni-directional and two-directional cyclic shears are shown in Figs. 3b and c, respectively.

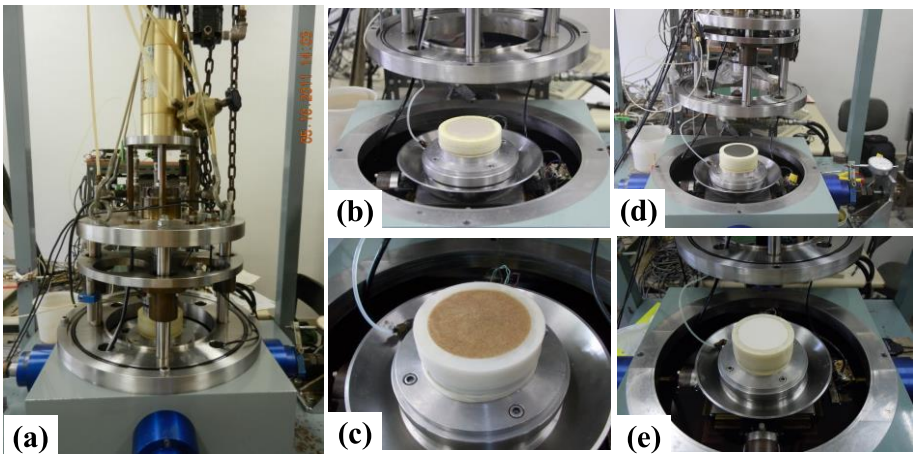

Figure 2. (a) Photo of the test apparatus; (b), (c), (d) and (e) situation of specimen of Nam O sand, Toyoura sand, Hue clay and Kaolin in the shear box, respectively

The cyclic shear strains from two orthogonal directions on horizontal plane (X and Y directions) can be simultaneously and independently applied by using the electro-hydraulic servo system while the vertical stress is automatically controlled by the aero-servo system. The shear strain amplitude γ is defined as a ratio of the maximum horizontal displacement (δ) to the initial height of specimen (h_o). In the uni-directional cyclic shear test, only one component of the shear strain in either X or Y direction, was applied to the specimen (e.g. only in X direction as seen in Fig. 3b) and in this case, the orbit of cyclic shear strain forms a linear line. Meanwhile for the two-directional test, two orthogonal components of the shear strain with various degrees of the phase difference were simultaneously applied to the specimen under the same shear strain amplitude (Fig. 3c). Then the orbit shows a linear line when $\theta = 0^o$, an elliptical line when $0^o < \theta < 90^o$ and a circle line for $\theta = 90^o$.

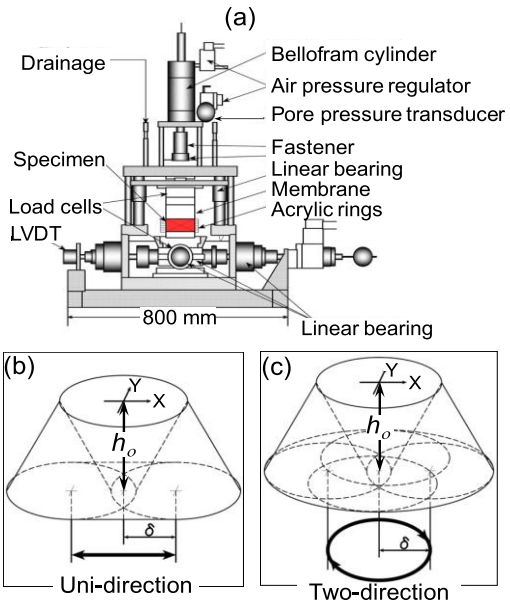

Figure 3. (a) Outline of the test device and deformation model of the specimen under (b) uni-directional and (c) two-directional cyclic shears

This study used two sandy soils, including Nam O and Toyoura sands, and two clayey

soils, including Hue and Kaolin clays, for the cyclic shear tests. Hue clay is a silty clay that partly constitutes the Phu Bai formation, and Nam O sand is the fine-grained sand of the Nam O formation. Hue clay is a dark-colored and weak organo-sedimentary soil characterized by high organic content and compressibility, low bearing capacity, and shear resistance (Nhan, 2004). Meanwhile, Nam O sand has low relative density and disadvantageous index properties to liquefaction resistance (Nhan, 2019). Besides widely spreading along the coastal plain in Thua Thien Hue and Quang Tri provinces, the soils also have changeable thickness and distribution depth and, in most case, extends close to the ground surface (Nhan, 2004; Thao, 2004; Vy, 2007). The map typically showing the distributions of Nam O sand and Hue clay has been presented by An et al. (2022).

Consequently, these soils have caused adverse effects on buildings' foundation stability and historical monuments' lifetime, as well as reducing technical and economic efficiencies of constructional operations in the areas (Thao, 2004; Nhan, 2019). Therefore, the dynamic properties of such soils have been observed in previous research in which information about the soils can be referred to in more detail (Nhan, 2019; Nhan and Matsuda, 2020; An et al., 2022; Nhan et al., 2022). Kaolin clay, a standardized clay, and Toyoura sand, a natural sand, are commonly used for laboratory testing in Japan (Lashkari, 2009; Matsuda et al., 2011; 2012). The grain size distribution curves of the soils are shown in Fig. 4, and several physico mechanical properties are summarized in Table 1.

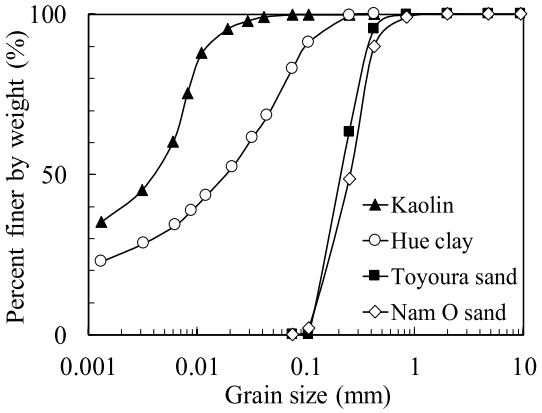

Figure 4. Grain size distribution curves of tested soils (results of Nam O sand and Hue clay were referred from An et al., 2022)

Table 1. Physico-mechanical properties of tested soils (results of Nam O sand and Hue clay were referred from An et al., 2022)

Properties	Nam O sand	Toyoura sand	Properties	Hue clay	Kaolin
Specific gravity, G_s	2.643	2.637	Specific gravity, G_s	2.68	2.71
Maximum void ratio, e_{max}	0.960	0.991	Liquid limit, w_L (%)	29.4	47.8
Minimum void ratio, e_{min}	0.653	0.630	Plastic limit, w_P (%)	18.7	22.3
Maximum dry density, ρ_{dmax} (g/cm^3)	1.599	1.617	Plasticity index, I_p	10.7	25.5
Minimum dry density, ρ_{dmin} (g/cm^3)	1.348	1.324	Compression index, C_c	0.20	0.31
Coefficient of uniformity, U_c	2.30	1.90			
Coefficient of curvature, U'_c	0.91	0.85	Swelling index, C_s	0.04	0.05
D_{60}; D_{50}; D_{30}; D_{10} (mm)	0.290; 0.255; 0.182; 0.126	0.240; 0.205; 0.160; 0.126			

The results in Fig. 4 and Table 1 indicate that Kaolin clay shows smaller grain size and higher Atterberg's limits than those of Hue clay, and therefore to clarify the effect of the Atterberg's limits on the dynamic properties of the soils, the same specimen preparation and testing condition should be used. Reconstituted samples of Hue and Kaolin clays were firstly mixed with de-aired water to form a slurry with a water content of about 1.5 times their liquid

limits (i.e., w = 44.1% and 71.7% for Kaolin and Hue clays, respectively). It is seen that Nam O sand has a mean particle size of D_{50} = 0.255 mm and a coefficient of uniformity of U_c = 2.30. Thus, this soil is classified as poorly-graded sand, being hard to compaction and vulnerable to liquefaction. Since Nam O and Toyoura sands have similar grain sizes and index properties (Fig. 4 and Table 1), specimens at different relative densities should be used to clarify the effects of this parameter on the dynamic behavior of the soils. In addition, the natural density of Nam O sand was confirmed in the range from 41% to 58.3% for the distribution depth from 0 m to 19.5 m (Hai, 2016; Hai et al., 2017; Tin, 2019; Nhan, 2019) and then, the specimen at D_r = 50% were prepared for Nam O sand while the specimen of Toyoura sand was fixed as D_r = 70%. Dried sand samples at predetermined volumes intended to produce D_r = 50% and 70% were mixed with de-aired water, so the sand was immersed in water. The slurry (of Hue and Kaolin clays) and sand-mixed water (of Nam O and Toyoura sands) were kept under constant water content for one day and de-aired in the vacuum cell before pouring into a rubber membrane in the Kjellman shear box of the test apparatus (Fig. 2). The slurry of clay and sand-mixed water were then consolidated under the vertical stress of σ_{vo} = 49 kPa. During the consolidation test, the vertical stress was automatically controlled at σ_{vo} = 49 kPa, and the pore water pressure was measured. The consolidation test is finished when the pore water pressure is dissipated (i.e., equal to zero). The records of vertical stress and the pore water pressure measurements during the consolidation test are typically shown in Fig. 5 for Kaolin clay (Nhan, 2013).

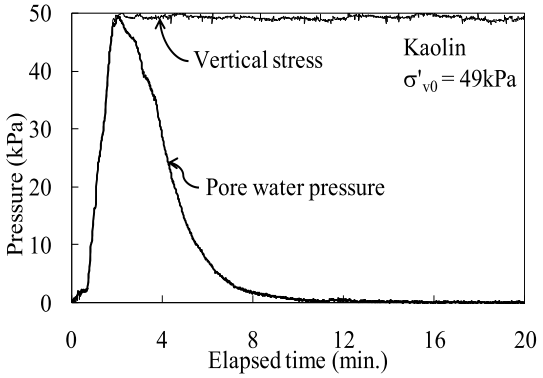

Figure 5. Typical records of the vertical stress and the pore water pressure during consolidation test before cyclic shearing (Nhan, 2013)

2.2. Test procedures and conditions

After the consolidation, the dimensions of the soil specimen are 75 mm in diameter and about 20 mm in height with an average void ratio of e = 0.73 and 1.15 for Hue clay and Kaolin, respectively, and with the relative density of Dr = 50% ± 5 and 70% ± 3% corresponding to Nam O and Toyoura sands. The soil specimen was then subjected to cyclic shear under undrained conditions. Since the saturation of Hue and Kaolin clays was confirmed by referring to the B-value ≥ 0.95, the undrained cyclic shear test was naturally carried out, and the cyclic shear-induced pore water pressure (u_{acc}) was measured by closing all drainages. In addition, the membrane-enclosed specimen was surrounded by a stack of acrylic rings (Figs. 2b-e) which permit cyclic simple shear deformation on the specimen under constant cross-sectional area. The aero-servo system automatically adjusted the vertical stress so that the height of the specimen was kept unchanged, and such a constant-volume condition was applied to Nam O and Toyoura sands. Since the decrement in the effective stress ($|\Delta\sigma'_v|$) under

constant-volume condition is equal to the increment in the pore water pressure (i.e., $|\Delta\sigma'_v| = u_{acc}$) under fully saturated condition, the similarity of these two conditions for simulating the undrained cyclic shear has been confirmed and widely applied to both sands and clays (Ishihara and Yamazaki, 1980; Matsuda et al., 2004; 2011; 2012; Nhan, 2013; Yasuhara and Andersen, 1991).

The waveform of the cyclic shear strain was sinusoidal with the frequency of f = 0.5 Hz (T = 2.0 s). The shear strain amplitude was changed from γ = 0.1% to 2.0%. The number of cycles was changed from n = 10 to 200 for sands and was fixed as n = 200 for clays. The cyclic shear direction includes uni-direction and two-direction, and for the two-directional cyclic shear, the phase difference (θ) was changed from 0° to 90° (called cyclic gyratory shear). Conditions of the undrained cyclic shear tests are summarized in Table 2.

Table 2. Conditions for undrained cyclic shear tests

Soil	Consolidation stress σ_{vo} (kPa)	Frequency f (Hz)	Number of cycles n	Uni-direction	Two-direction	
				Shear strain amplitude γ(%)	Phase difference θ (°)	Shear strain amplitude γ(%)
Hue clay	49	0.5	200	0.05 - 1.0	45°, 90°	0.1 - 1.0
Kaolin				0.1 - 2.0	20°, 45°, 70°, 90°	0.1 - 2.0
Nam O sand			10 - 150	0.1 - 2.0	0°, 45°, 90°	0.1 - 1.0
Toyoura sand			15 - 200	0.1 - 1.0		

3. Results and discussions

3.1. Changes in effective stress of sands and pore water pressure of saturated clays during undrained cyclic shears

As mentioned previously, the effective stress (σ'_v) in Nam O and Toyoura sands decreases during the constant-volume cyclic shearing, equal to the increase in the pore water pressure in Hue clay and Kaolin (i.e. $|\Delta\sigma'_v| = u_{acc}$). The changes of σ'_v and u_{acc} are typically shown in Fig. 6 for Nam O sand and Kaolin subjected to undrained uni-directional and two-directional cyclic shears at the shear strain amplitude γ = 0.1%, 0.4% and 1.0%.

It is seen that σ'_v decreases and u_{acc} increases during the undrained cyclic shear (*i.e.* with the number of cycles n) and that the larger the amplitude of the cyclic shear, the quicker the decrease in σ'_v on Nam O sand and the increase in u_{acc} on Kaolin. Since $\sigma_{vo} = \sigma'_v + u_{acc}$ and when σ'_v equals to zero ($\sigma'_v = 0$) meaning that u_{acc} equals to the initial vertical stress (i.e. $u_{acc} = \sigma_{vo}$ = 49 kPa), then the soil is liquefied. It is seen in Fig. 6 that liquefaction occurs on Nam O sand meanwhile this condition is not reached on Kaolin even after a relatively large cycle number (n = 200). In addition, the cyclic shears with larger γ (γ = 0.4% and 1.0%) result in sudden decreases in σ'_v and consequently, liquefaction occurs on Nam O sand after several cycles. Comparisons of the results between Figs. 6a and b indicate that at the same n and γ, the two-directional cyclic shear (θ = 90° in Fig. 6b) induces quicker decreases in σ'_v and increases in u_{acc} than those under the uni-directional one. Due to the relation of $|\Delta\sigma'_v| = u_{acc}$ and for simplifying the remaining content, the terms of pore water pressure accumulation u_{acc} should be used for both undrained conditions (An et al., 2022).

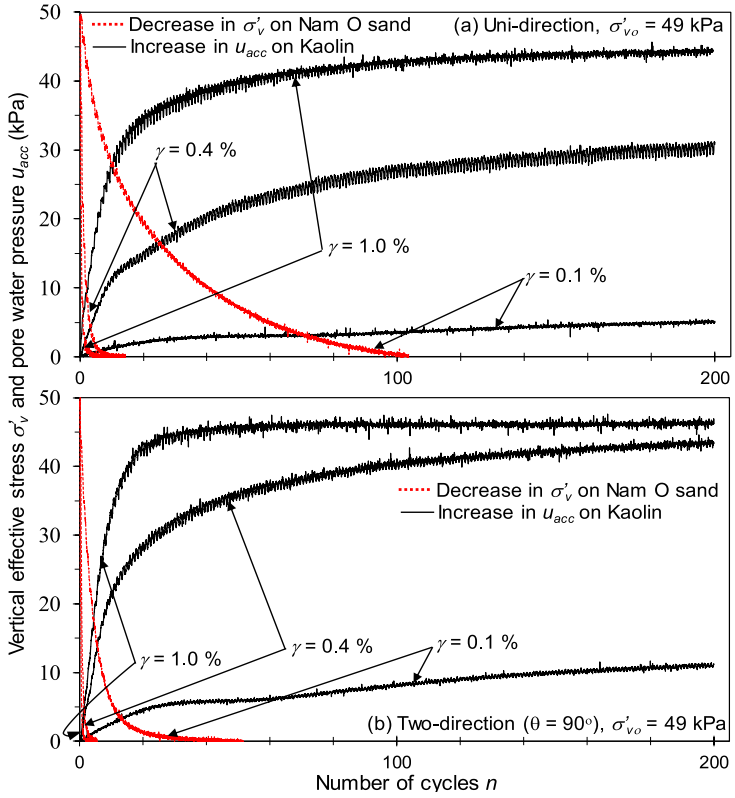

Figure 6. Typical decreases in σ'_v on Nam O sand and increases in u_{acc} on Kaolin during undrained cyclic shearing with different amplitudes and directions ((a) uni-direction and (b) two-direction at $\theta = 90^o$)

3.2. Considering the pore water pressure responses of saturated soils using conventional parameters

To show the pore water pressure accumulation from the beginning to the end of the cyclic shear, the pore water pressure ratio, defined by u_{acc}/σ'_{vo} where σ'_{vo} is the initial effective stress, are plotted against the logarithm of n for all soils as seen in Fig. 7. In Fig. 7a, several experiments at the same conditions (cyclic shear direction and γ) were performed on Toyoura sand and the obtained agreements confirm the precision of the testing results. It is seen in Fig. 7 that the pore water pressure ratio u_{acc}/σ'_{vo} increases with n, and at the same n, cyclic shear tests at larger γ result in higher u_{acc}/σ'_{vo}. At the same n and γ, the two-directional cyclic shear induces the higher u_{acc}/σ'_{vo}. The discrepancy of u_{acc}/σ'_{vo} between the uni-directional and two-directional cyclic shears reveals the effect of the cyclic shear direction on the cyclic shear-induced pore water pressure accumulation of saturated soils. For Nam O and Toyoura sands (Figs. 7a, b), the discrepancies of u_{acc}/σ'_{vo} are evident at γ= 0.1%, tend to decrease with γ, and become negligible when γ = 1.0%. For Hue and Kaolin clays (Figs. 7c, d), such discrepancies, even become largest at γ= 0.2%-0.4% and still remain at γ= 1.0% and n = 200, show more complicated variation with n and γ. Matasovic and Vucetic (1992, 1995) indicated that the cyclic resistance and degradation of soils are significantly related to and affected by cyclic shear-induced pore water pressure accumulation. Therefore, the higher u_{acc}/σ'_{vo} in Figs. 7a-d suggests the higher disturbance and degradation of the soils when subjected to the two-directional cyclic shear.

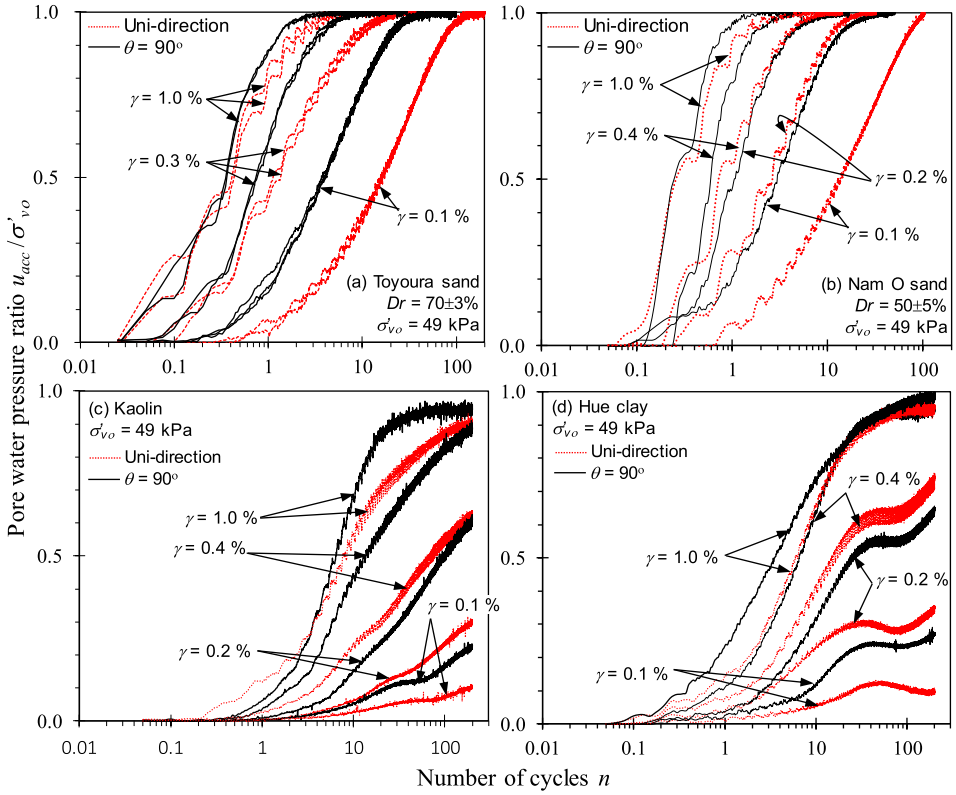

Figure 7. Changes of u_{acc}/σ'_{vo} on (a) Toyoura sand, (b) Nam O sand, (c) Kaolin clay and (d) Hue clay subjected to undrained cyclic shearing with different conditions

To show the effects of the relative density of sands and Atterberg's limits of clays on the cyclic shear-induced pore water pressure property, the results of u_{acc}/σ'_{vo} in Figs. 7a-d are compared between sands and clays under the same testing conditions as shown in Figs. 8 and 9. It is seen that Toyoura sand at higher density and Kaolin with higher Atterberg's limits show a slower rate of the pore water pressure accumulation and consequently, at the same n, obtained values of u_{acc}/σ'_{vo} on Toyoura sand and Kaolin are lower than those on Nam O sand and Hue clay, respectively. Based on the cyclic shear test results on normally and over-consolidated clays and sands, Vucetic and Dobry (1991) indicated that the Atterberg's limits (namely the plasticity index) importantly govern the dynamic behavior of soil deposits and that the higher the Atterberg's limits of fine-grained soil, the lower the stiffness degradation at an arbitrary amplitude of the cyclic shear strain. Therefore, based on the obtained results of the pore water pressure accumulation, Toyoura sand at higher density and Kaolin clay with higher Attergber's limits show higher cyclic resistance than those of Nam O sand at lower density and Hue clay with lower Atterberg's limits, respectively and such an observation is confirmed for both uni-directional and two-directional cyclic shears.

3.3. Threshold number of cycles for pore water pressure generation on saturated sands and clays

By plotting the results of u_{acc}/σ'_{vo} against the logarithm of n as shown in Figs. 7-9, the changes in the pore water pressure can be described from the beginning to the end of the

cyclic shearing, and since $\gamma > \gamma_{tp}$ (i.e. the smallest γ = 0.1% used in this study and therefore being larger than γ_{tp} = 0.024%-0.06% and γ_{tp} = 0.01%-0.02% as previously mentioned for clay and sand, respectively), the pore water pressure is quickly generated after the application of the cyclic shear strain. It is seen in these figures that, for each soil, the number of cycles at which the pore water pressure starts to generate (i.e. u_{acc}/σ'_{vo} becomes >0) decreases with γ. This parameter was referred to as the threshold number of cycles for cyclic shear-induced pore water pressure generation, symbolized as n_{tp}. n_{tp} was generally mentioned for clays and sands (Nhan et al., 2012; Nhan, 2013; Nhan and Matsuda, 2020) and recently determined in more detail for Hue clay and Nam O sand subjected to uni-directional and two-directional cyclic shears (An et al., 2022). Therefore, in this study, n_{tp} should be determined for Toyoura sand and Kaolin subjected to the same cyclic shearing conditions so that the effects of the soil properties and cyclic shearing conditions can be considered.

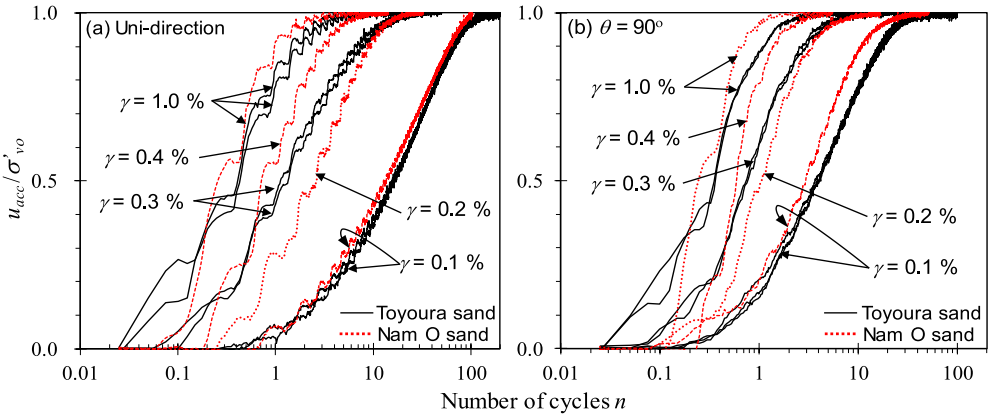

Figure 8. Comparison of relations between u_{acc}/σ'_{vo} and n on saturated sands subjected to undrained cyclic shear with different amplitudes and directions ((a) uni-direction and (b) two-direction at $\theta = 90^o$)

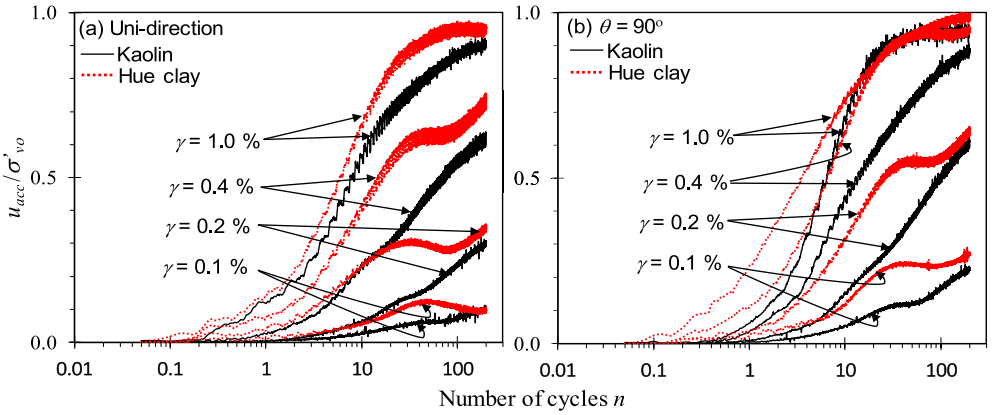

Figure 9. Comparison of relations between u_{acc}/σ'_{vo} and n on saturated clays subjected to undrained cyclic shear with different amplitudes and directions ((a) uni-direction and (b) two-direction at $\theta = 90^o$)

Obtained results of n_{tp} on Toyoura sand and Kaolin (symbolized as n_{tpTO} and n_{tpKAO}, respectively) are summarized in Table 3. Changes of this parameter with γ are shown in Fig. 10. In Table 3 and Fig. 10, the results of n_{tp} on Nam O sand and Hue clay (symbolized as n_{tpNO} and n_{tpHU}, respectively) were referred from previous research (An et al., 2022) in

which method for determination of n_{tp} was described in detailed. The observations indicate that n_{tp} generally decreases with γ regardless of the types of soils and the cyclic shear direction. In addition, when comparing n_{tp} between the soils under the same cyclic shearing conditions, Toyoura sand at higher relative density shows smaller n_{tp} than those of Nam O sand at lower density (Fig. 10a). Meanwhile, in Fig. 10b, Kaolin with higher Atterberg's limits shows higher n_{tp} compared with that of Hue clay.

Table 3. Obtained results of n_{tp} for saturated soils subjected to undrained cyclic shear with different amplitudes and directions

Shear direction	Uni-direction				$\theta = 90^o$			
Soil \ γ (%)	0.1	0.2	0.4	1.0	0.1	0.2	0.4	1.0
Nam O sand (n_{tpNO}) (*)	0.63	0.25	0.2	0.075	0.44	0.31	0.27	0.15
Hue clay (n_{tpHU}) (*)	0.15	0.125	0.075	0.05	0.175	0.15	0.125	0.05
Kaolin (n_{tpKAO})	0.15	0.98	0.22	0.11	0.45	0.43	0.40	0.14
Toyoura sand (n_{tpTO})	0.26 0.425	0.055 (**) 0.081 (**)		0.025 0.027	0.05 0.09 0.12	0.047 (**) 0.035 (**)		0.026 0.026

(*) Results of Nam O sand and Hue clay were referred from An et al. (2022). (**) The results obtained for γ = 0.3%

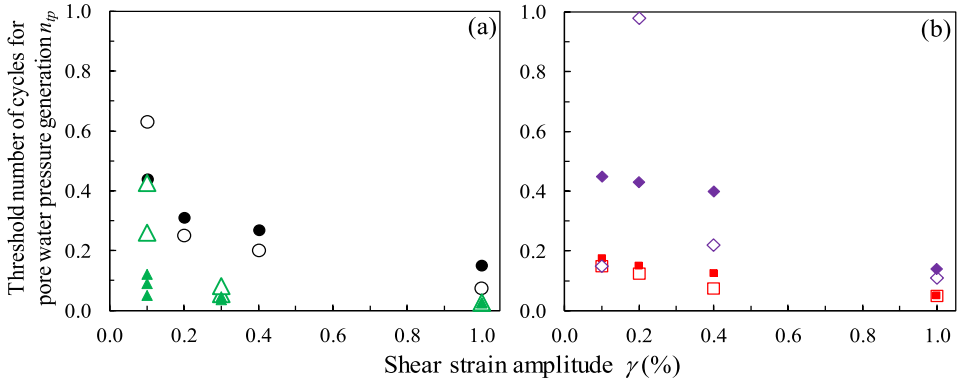

Figure 10. Changes of n_{tp} with γ for (a) sandy soils and (b) clayey soils subjected to uni-directional and two-directional cyclic shears (obtained results on Nam O sand and Hue clay were referred from An et al., 2022)

3.4. Threshold cumulative shear strain for pore water pressure generation on saturated sands and clays

To show the changes of u_{acc}/σ'_{vo} with the cumulative shear strain G^*, which is a new strain path parameter, the observed results in Figs. 8 and 9 are shown again in Figs. 11, 12, respectively. G^* in these figures was determined by applying Eq. (1) proposed by Fukutake and Matsuoka (1989). The advantage of this parameter in simulating the cyclic shear-induced pore water pressure accumulation during undrained cyclic shear has been thoroughly analyzed in previous research (Matsuda et al., 2011; 2012; 2013; Nhan, 2013; Sato et al., 2018).

$$G^* = \Sigma \Delta G^* = \Sigma (\Delta\gamma_x^2 + \Delta\gamma_y^2)^{0.5} \quad (1)$$

Where $\Delta\gamma_x$ and $\Delta\gamma_y$ are the shear strain increment in two orthogonal directions, *i.e.*, X and Y directions, respectively.

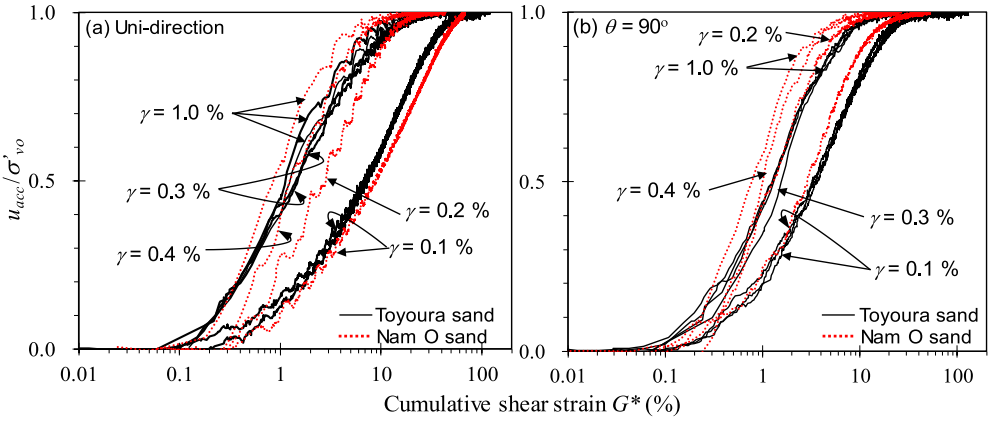

Figure 11. Comparison of the relations between u_{acc}/σ'_{vo} and G^* on saturated sands subjected to undrained cyclic shear with different amplitudes and directions ((a) uni-direction and (b) two-direction at $\theta = 90^o$)

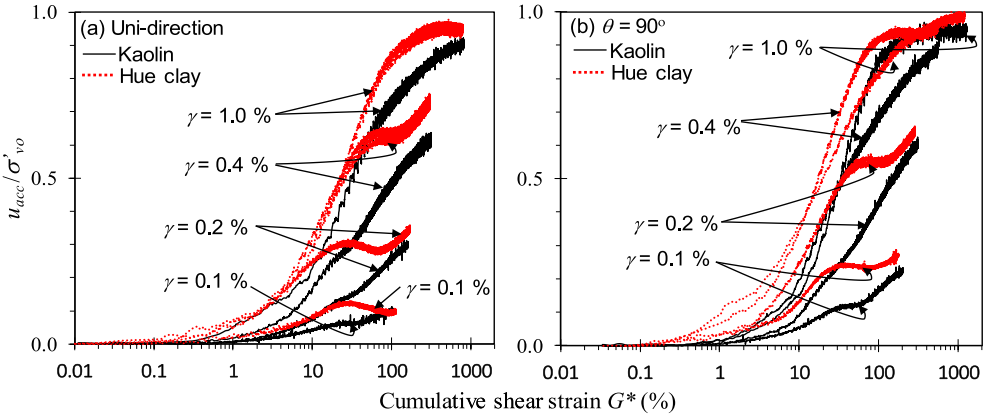

Figure 12. Comparison of the relations between u_{acc}/σ'_{vo} and G^* on saturated clays subjected to undrained cyclic shear with different amplitudes and directions ((a) uni-direction and (b) two-direction at $\theta = 90^o$)

Eq. (1) indicates that G^* denotes the summation of the shear strain increment during cyclic shearing, or this parameter denotes the length along the shear strain path and is related to the cyclic shear-induced disturbance of soil structure. This means that the cyclic shear with a longer application (i.e., larger number of cycles) and a larger amplitude (i.e., γ) results in a larger value of G^*. For the case of Hue and Kaolin clays which are not liquefied as seen in Fig. 12 and all cyclic shear tests were fixed at $n = 200$, the cyclic shear at larger γ induces the larger values of G^* and the larger G^* results in the higher u_{acc}/σ'_{vo}. Meanwhile, the tendencies are different for Toyoura and Nam O sands, which were liquefied, as seen in Fig. 11. It is interestingly indicated that by using G^* instead of n (as shown in Fig. 8), the changes in u_{acc}/σ'_{vo} become more unique. When $\gamma > 0.3\%$, the discrepancies of u_{acc}/σ'_{vo} become negligible regardless of the shear strain amplitude and shear direction. Therefore, G^* can be used to capture the effect of the shear

strain amplitude and shear direction on the pore water pressure accumulation of saturated sands subjected to undrained cyclic shears.

Using the plots in Figs. 11 and 12, the threshold cumulative shear strain for pore water pressure generation, symbolized by G^*_{tp} and similarly defined as n_{tp} can be obtained for Toyoura sand and Kaolin (symbolized as G^*_{tpTO} and G^*_{tpKAO}, respectively) under different cyclic shearing conditions. Obtained results of G^*_{tpTO} and G^*_{tpKAO} are summarized in Table 4 and plotted against γ in Fig. 13. The results of G^*_{tp} on Nam O sand and Hue clay (symbolized as G^*_{tpNO} and G^*_{tpHU}, respectively) were referred from previous research (An et al., 2022) in which the method for determination of G^*_{tp} was also described in detail. In Fig. 13a, despite several scattering on G^*_{tpNO}, the results of G^*_{tp} are mainly in the range from 0% to 0.1%. Therefore, G^*_{tp} = 0.1% can be considered a criterion value for pore water pressure generation in sands. Meanwhile, in Fig. 13b, G^*_{tpHU} and G^*_{tpKAO} generally decrease with γ, and Kaolin with higher Atterberg's limits shows higher G^*_{tp} (i.e., G^*_{tpKAO}>G^*_{tpHU}). Since the decreasing tendency of G^*_{tpHU} and G^*_{tpKAO} are not clear and scattering on G^*_{tpKAO} is remained, uni-directional and two-directional cyclic shear tests should be further carried out on other clays.

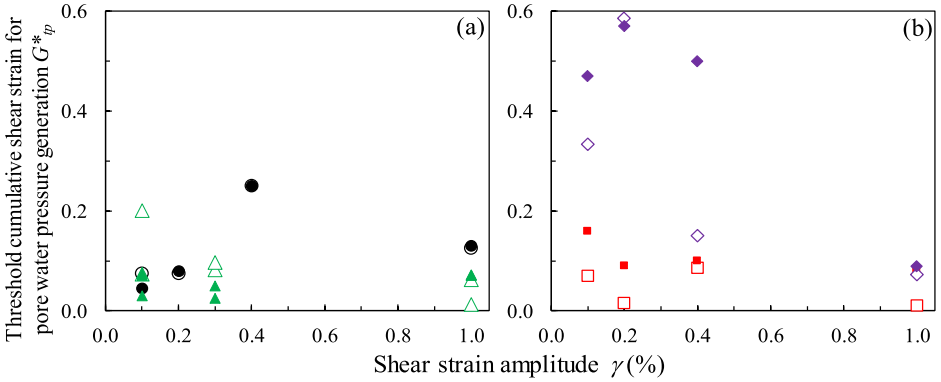

Figure 13. Changes of G^*_{tp} with g for (a) sandy soils and (b) clayey soils subjected to uni-directional and two-directional cyclic shears (obtained results on Nam O sand and Hue clay were referred from An et al., 2022)

Table 4. Obtained results of G^*_{tp} for saturated soils subjected to undrained cyclic shear with different amplitudes and directions

Shear direction	Uni-direction				θ= 90°			
Soil / γ (%)	0.1	0.2	0.4	1.0	0.1	0.2	0.4	1.0
Nam O sand (G^*_{tpNO}) (*)	0.075	0.075	0.25	0.125	0.045	0.08	0.25	0.13
Hue clay (G^*_{tpHU}) (*)	0.07	0.016	0.086	0.01	0.16	0.09	0.1	0.08
Kaolin (G^*_{tpKAO})	0.333	0.585	0.15	0.072	0.47	0.57	0.5	0.089
Toyoura sand (G^*_{tpTO})	0.073 0.20	0.082 (**) 0.096 (**)		0.062 0.0125	0.03 0.07 0.074	0.025 (**) 0.049 (**)		0.07 0.072

(*) Results of Nam O sand and Hue clay were referred from An et al. (2022). (**) The results obtained for γ = 0.3%

3.5. Comparisons of u_{acc}/σ'_{vo} between sands and clays for different cyclic shear conditions

The changes of u_{acc}/σ'_{vo} with γ are shown by symbols in Fig. 14(a) for different soils and cyclic shearing conditions used in this study. For Toyoura and Nam O sands which were subjected to cyclic shear tests with different number of cycles, the results become scattering, and therefore, several results were typically noticed by arrows to show the effect of this parameter on u_{acc}/σ'_{vo}. It is seen that when $\gamma \leq 0.3\%$, the undrained cyclic shears with larger n and with two-direction induce the higher u_{acc}/σ'_{vo} suggesting the effects of these parameters on the pore water pressure accumulation of sands. However, when $\gamma > 0.3\%$, Toyoura and Nam O sands are quickly liquefied; therefore, such effects become negligible. For Kaolin and Hue clays subjected to cyclic shear tests with the same n (i.e., $n = 200$), the two-directional cyclic shears induce higher u_{acc}/σ'_{vo} than those generated by the uni-directional one, and such an effect of the cyclic shear direction remains at $\gamma = 1.0\%$. The results of u_{acc}/σ'_{vo} in Fig. 14a are shown against G^* in Fig. 14b, and it is seen that by using G^* instead of γ, the increasing tendencies of u_{acc}/σ'_{vo} become unique on each soil regardless of the cyclic shear direction, shear strain amplitude and the number of cycles. Consequently, fitting lines can be referred to promote a prediction of the pore water pressure accumulation for the soils used in this study. When comparing the results between sands and clays for the same G^*, Toyoura sand with higher density and Kaolin with higher plasticity show smaller u_{acc}/σ'_{vo} than those on Nam O sand and Hue clay, respectively. These observations indicate that G^* can be advantageously used to capture the effects of the cyclic shear conditions on the pore water pressure accumulation of sands and clays; meanwhile, with this parameter, the effects of the relative density of sands and the Atterberg's limits of clays can not be eliminated.

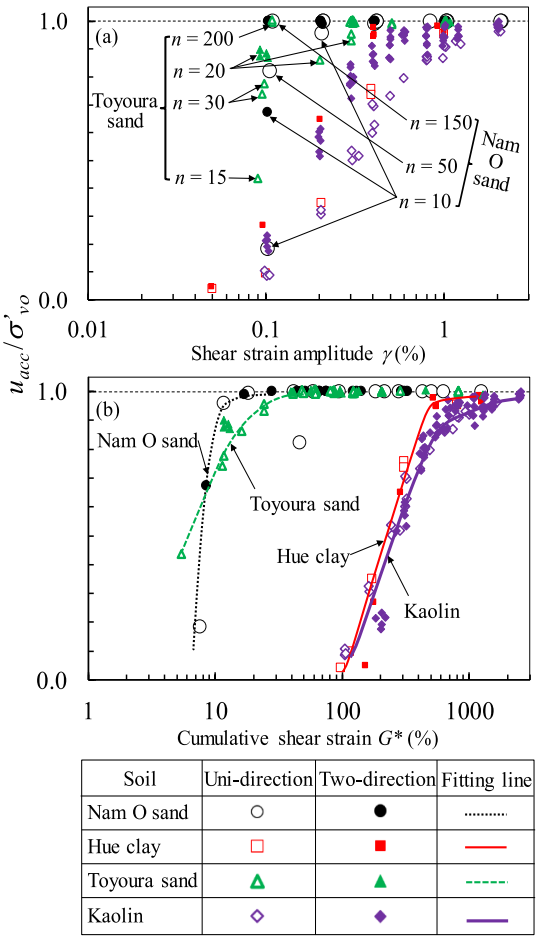

Soil	Uni-direction	Two-direction	Fitting line
Nam O sand	○	●	·····
Hue clay	□	■	——
Toyoura sand	△	▲	- - - -
Kaolin	◇	◆	——

Figure 14. Relations of u_{acc}/σ'_{vo} versus (a) the shear strain amplitude γ and (b) the cumulative shear strain G^* for different soils and undrained cyclic shear conditions (obtained results on Nam O sand and Hue clay were referred from An et al., 2022)

4. Conclusions

The main conclusions are as follows:

(1) When subjected to the same undrained cyclic shear conditions, sandy soil at higher relative density and clay with higher Atterberg's limits show a slower rate of pore water pressure accumulation resulting in a lower ratio of the cyclic shear-induced pore

water pressure. For sandy soils, which are easily liquefied under undrained cyclic loading, the effects of cyclic shear direction and shear strain amplitude become negligible when $\gamma \geq 0.3\%$, whereas for clay with higher liquefaction resistance, such effects remain even at $\gamma = 1.0\%$ and $n = 200$.

(2) The threshold number of cycles for pore water pressure generation generally decreases with γ regardless of the soil type and cyclic shear direction. For sandy soils which have similar index properties, Toyoura sand at higher D_r shows smaller n_{tp} (i.e., $n_{tpTO} < n_{tpNO}$) meanwhile, for clay, Kaolin with higher Atterberg's limits shows higher n_{tp} (i.e., $n_{tpKAO} > n_{tpHU}$).

(3) As to the threshold cumulative shear strain for pore water pressure generation, the values of G^*_{tp} obtained on Nam O and Toyoura sands mainly change in the range from 0% to 0.1%. Therefore, $G^*_{tp} = 0.1\%$ can be considered as a criterion for pore water pressure generation in sands. For Kaolin and Hue clays, despite several scattering on Kaolin, G^*_{tp} generally decreases with γ, and Kaolin with higher Atterberg's limits shows higher values of G^*_{tp} (i.e., $G^*_{tpKAO} > G^*_{tpHU}$).

(4) The effects of shear strain amplitude and cyclic shear direction on the pore water pressure accumulation of saturated sands and clays can be eliminated by using G^*. Consequently, relations of u_{acc}/σ'_{vo} versus G^* become unique on each soil. Therefore, empirical fitting lines can be used to predict the pore water pressure accumulation of the used soils subjected to undrained uni-directional and two-directional cyclic shears.

(5) Even with the application of G^*, the discrepancies of u_{acc}/σ'_{vo} are seen between sandy specimens at different densities and between clays at different Atterberg's limits indicating that the effects of the relative density and the Atterberg's limits on the pore water pressure accumulation of the soils remain.

Acknowledgments

This research is funded by Hue University under the Core Research Program, Grant No. NCM.DHH.2018.03 and by Vietnam National Foundation for Science and Technology Development (NAFOSTED) under Grant Number 105.08-2018.01. The experimental works were supported by students who graduated Yamaguchi University. The authors would like to express their gratitude to them.

References

An T.T.P., Matsuda H., Nhan T.T., Nhan N.T.T., Tien P.V., Thien D.Q., 2022. Pore water pressure responses of saturated sand and clay under undrained cyclic shearing. Vietnam Journal of Earth Sciences, 44(2), 181-194.

Dobry R., Powell D., Yokel F.Y., Ladd R.S., 1980. Liquefaction potential of saturated sand-The stiffness method. 7th World Conference on Earthquake Engineering, 3, 25-32.

Dobry R., Ladd R.S., Yokel R.Y., Chung R.M., 1982. Prediction of pore water pressure buildup and liquefaction of sands during earthquakes by cyclic strain method. National Bureau of Standards Building Science, Series 138, Washington D.C.

Dobry R., Pierce W.G., Dyvik R., Thomas G.E., Ladd R.S., 1985. Pore pressure model for cyclic straining of sand. Research Report, Civil Engineering Department, Rensselaer Polytechnic Institute, Troy, New York.

Fukutake K., Matsuoka H.A., 1989. Unified law for dilatancy under multi-directional simple shearing. Journal of JSCE Division C, JSCE, 412(III-1), 143-151.

Hai L.D., 2016. Study on the liquefaction potential of sandy soils constituting of Nam O formation along the coastal plain of Quang Tri province. Master Thesis. Hue University of Sciences, Vietnam, 72p.

Hai L.D., Nhan T.T., Huong H.T.S., 2017. Liquefaction potential and post-liquefaction settlement of fine-grained sand constituting of Nam O formation along Quang Tri coastal plain. Hue Univ. Journal of Science: Earth Science and Environment, 126(4A), 49-60.

Hsu C.C., Vucetic M., 2006. Threshold shear strain for cyclic pore-water pressure in cohesive soils. Journal of Geotechnical and Geoenvironmental Engineering, 132(10), 1325-1335.

Ishihara K., Yamazaki F., 1980. Cyclic simple shear tests on saturated sand in multi-directional loading. Soils and Foundations, 20(1), 45-59.

Lashkari A., 2009. A constitutive model for sand liquefaction under rotational shear. Iranian Journal of Science and Technology Transaction B: Engineering, 33, 31-48.

Matsuda H., Ohara S., 1989. Threshold strain of clay for pore pressure buildup. 12th World Conference on Soil Mechanics and Foundation Engineering, 127-130.

Matsuda H., Hoshiyama E., Ohara S., 1991. Settlement calculations of clay layers induced by earthquake. 2nd International Conference on Recent Advances in Geotechnical Earthquake Engineering and Soil Dynamics, 473-479.

Matsuda H., Shinozaki H., Okada N., Takamiya K., Shinyama K., 2004. Effects of multi-directional cyclic shear on the post-earthquake settlement of ground. 13th world conference on earthquake engineering, 2890, 1-10.

Matsuda H., Andre P.H., Ishikura R., Kawahara S., 2011. Effective stress change and post-earthquake settlement properties of granular materials subjected to multi-directional cyclic simple shear. Soils and Foundations, 51(5), 873-884.

Matsuda H., Nhan T.T., Ishikura R., Inazawa T., 2012. New criterion for the liquefaction resistance under strain-controlled multi-directional cyclic shear. 15th World Conference on Earthquake Engineering (15WCEE), 4149, 1-10.

Matsuda H., Nhan T.T., Ishikura R., 2013. Prediction of excess pore water pressure and post-cyclic settlement on soft clay induced by uni-directional and multi-directional cyclic shears as a function of strain path parameters. Soil Dynamics and Earthquake Engineering, 49, 75-88.

Matsuda H., Nhan T.T., Sato H., Thien D.Q., Tuyen T.H., Nhan N.T.T., 2015. Threshold shear strain for pore water pressure buildup of clays subjected to uni-directional and multi-directional cyclic shears focused on static loading history and plasticity index. The 2nd International Conference on Engineering geology in Respond to Climate Change and Sustainable Development of Infrastructure (Hanoi Geo 2015), 177-186.

Matsui T., Ohara H., Ito T., 1980. Cyclic stress-strain history and shear characteristics of clay. Journal of Geotechnical Engineering, ASCE, 106(GT10), 1101-1120.

Nhan N.T.T., 2004. Study on physico-machenical properties of Phu Bai formation along Thua Thien-Hue coastal plain and proposal of improvement solution using sand compaction pile method. Master Thesis. Hue University of Sciences, Vietnam, 93p.

Nhan T.T., Matsuda H., Thien D.Q., Tuyen T.H., An T.T.P., 2012. New criteria for cyclic failure of normally consolidated clays and sands subjected to uniform and irregular cyclic shears. The International Workshop on Geo-Engineering for Responding to Climate Change and Sustainable Development of Infrastructure (Hue Geo-Engineering 2012), 127-138.

Nhan T.T., 2013. Study on excess pore water pressure and post-cyclic settlement of normally consolidated clay subjected to uniform and irregular cyclic shears. Doctoral dissertation, Yamaguchi University, Japan, 131p.

Nhan T.T., 2019. Liquefaction resistance and post-cyclic settlement of Nam O sand subjected to uni-directional and multi-directional cyclic shears. Lecture Notes in Civil Engineering, 18, 102-107.

Nhan T.T., Matsuda H., 2020. Pore water pressure accumulation and settlement of clays with a wide range of Atterberg's limits subjected to multi-directional cyclic shear. Vietnam Journal of Earth Sciences, 42(1), 2615-9783.

Nhan T.T., Matsuda H., An T.T.P. 2022. Effective stress change and cyclic resistance of saturated sands under uniform and irregular cyclic shears. Indian Geotechnical Journal, 52(3), 507-518.

Ohara S., Matsuda H., 1987. Settlement of saturated clay layer induced by cyclic shear. 9th Southeast Asia Geotechnical Conference, 713-722.

Ohara S., Matsuda H., 1988. Study on the settlement of saturated clay layer induced by cyclic shear. Soils and Foundations, 28(3), 103-113.

Pyke R., Seed H.B., Chan C.K., 1975. Settlement of sands under multidirectional shaking. Journal of Geotechnical Engineering, ASCE, 101(GT4), 379-398.

Sato H., Nhan T.T., Matsuda H., 2018. Earthquake-induced settlement of a clay layer. Soil Dynamics and Earthquake Engineering, 104, 418-431.

Silver M.L., Seed H.B., 1971. Volume changes in sands during cyclic loading. Journal of the Soil Mechanics and Foundations Division, ASCE, 97(SM9), 1171-1182.

Thao P.T., 2004. Study on types of soil profiles in Hue city and proposal of suitable technical solutions for soil improvement. Master thesis, Hue University of Sciences, Vietnam, 88p.

Tin T.N., 2019. Assessment of the liquefaction resistance of sandy soils in Quang Tri coastal plain based on standard penetration test and cyclic shear test. Master thesis, Hue University of Sciences, Vietnam, 69p.

Vucetic M.A., Dobry R., 1991. Effect of soil plasticity on cyclic response. Journal of Geotechnical Engineering, ASCE, 117(1), 89-107.

Vy T.T.B., 2007. Establishment of the engineering geological map at large scale for Hue city and surrounding areas. Master thesis, Hue University of Sciences, Vietnam, 78p.

Yasuhara K., Andersen K.H., 1991. Recompression of normally consolidated clay after cyclic loading. Soils and Foundations 31(1), 83-94.

Youd L.T., 1972. Comparison of sands by repeated shear straining. Journal of the Soil Mechanics and Foundations Division, ASCE, 98(SM7), 709-725.